ISIJ International, Vol. 42 (2002), No. 12, pp. 1565–1570

Thermal and Mechanical Stability of Retained Austenite in Aluminum-containing Multiphase TRIP Steels

Sybrand van der ZWAAG, Lie ZHAO, Suzelotte O. KRUIJVER and Jilt SIETSMA[1)]

Netherlands Institute for Metals Research, Rotterdamseweg 137, 2628 AL Delft, The Netherlands; also at Laboratory for Materials Science, Delft University of Technology, Rotterdamseweg 137, 2628 AL Delft, The Netherlands. Email: L.Zhao@tnw.tudelft.nl 1) Laboratory for Materials Science, Delft University of Technology, Rotterdamseweg 137, 2628 AL Delft, The Netherlands

(*Received on July 10, 2002; accepted in final form on September 24, 2002*)

Stability of retained austenite is the key issue to understand transformation-induced plasticity (TRIP) effect. In this work, both thermal stability and mechanical stability are investigated by thermo-magnetic as well as *in situ* conventional X-ray diffraction and micro synchrotron radiation diffraction measurements. The thermal stability in a 0.20C–1.52Mn–0.25Si–0.96Al (wt%) TRIP steel is studied in the temperature range between 5 and 300 K under a constant magnetic field of 5 T. It is found that almost all austenite transforms thermally to martensite upon cooling to 5 K and M_S and M_f temperatures are analyzed to be 355 and 115 K. Transformation kinetics on the fraction *versus* temperature relation are well described by a model based on thermodynamics. From the *in situ* conventional X-ray and synchrotron diffraction measurements in a 0.17C–1.46Mn–0.26Si–1.81Al (wt%) steel, the volume fraction of retained austenite is found to decrease as the strain increases according to Ludwigson and Berger relation. The diffraction measurements also show that the mechanical stability depends on the orientation of the grain with respect to the direction of the applied stress, and the austenite grains at an angle of 45° or 60° were found to be more stable than those at lower or higher angles. Both thermal and diffraction experiments show an increase in the average carbon concentration of the remaining austenite with lowering temperature or increasing stress. Thermal and mechanical stability of retained austenite is therefore attributed to the carbon distribution over different austenite grains.

KEY WORDS: TRIP steel; retained austenite; martensitic transformation; X-ray diffraction; thermo-magnetization; synchrotron.

1. Introduction

Low-alloyed multiphase transformation-induced plasticity (TRIP) steels have attracted a growing interest in recent years due to their high strength and enhanced formability.[1,2)] These excellent mechanical properties mainly arise from a martensitic transformation of metastable retained austenite under the influence of external tensile stress. Detailed insight in the stability range of retained austenite is thus regarded to be of the highest importance for controlling the materials properties. Numerous modelings[3,4)] and experiments[5–9)] show that the factors influencing the stability of retained austenite in TRIP steels include the chemical composition in austenite,[6,7)] size[4,5)] and shape[9)] of the grain and dislocation density,[8)] *etc*. In the present study, the effect of carbon concentration in retained austenite is highlighted. This is due to the fact that during thermal process of the TRIP steels significant inhomogeneity of the carbon distribution in austenite is introduced. As reported,[9–12)] the austenite could be retained along the bainite–ferrite boundary (so-called intergranular austenite), inside ferritic grains (inter-ferritic austenite) or between bainitic plates (interlath film-like austenite).[9)] The inter-ferritic austenite would have a lower carbon concentration than the intergranular or interlath austenite since it is probably formed during intercritical annealing[13)] and carbon enrichment occurs during subsequent cooling. It is understandable that the interlath film-like retained austenite has a higher carbon concentration than the intergranular austenite because it is enriched from both sides of the bainite plates.

From the macroscopic point of view, it has been widely found that the austenite volume fraction in TRIP steels decreases with increasing the strain during tensile test. To describe the relation between the fraction of retained austenite (f^γ) and strain (ε), Matsumura *et al*.[14)] analyzed f^γ *versus* ε data using the Austin and Rickett type of equation.[15–18)] They found that the autocatalytic effect, *i.e*. the ability of martensite to accelerate the formation of additional martensite, in TRIP steels and dual phase steels is suppressed due to a large amount of ferrite or bainite acting as barriers against the autocatalytic propagation. Therefore, the f^γ *versus* ε relation is as follows

$$1/f^\gamma - 1/f_0^\gamma = k\varepsilon \quad \ldots\ldots (1)$$

where f_0^γ is the initial volume fraction of retained austenite and k the constant regarding as a measure for the mechanical stability of retained austenite. As the engineering strain is used in this paper,[17] the above relation is thus called the Ludwigson and Berger equation.

The strain dependence of the austenite fraction, from which the mechanical stability of retained austenite can be determined, was usually determined by X-ray diffraction (XRD) in the samples unloading at different strain levels.[6,7,19] In the present work, the austenite fraction was determined under stress condition. To clarify the effect of orientation between the applied stress and the diffraction planes, the *in situ* XRD measurements are also performed using synchrotron radiation diffraction technique. On the other hand, no work on the thermal stability of retained austenite in TRIP steels has been reported, although such studies can give useful information on the stability of retained austenite grains. The thermal martensitic transformation of retained austenite in TRIP steels is thus also measured in the present work.

2. Experimental Procedure

Two Al-containing low-alloyed multiphase TRIP steels, Al1.8 grade and Al1.0 grade, were used in this work and their main compositions are shown in **Table 1**. The materials were machined to tensile samples for *in situ* tensile tests or to cylindrical samples for the thermo-magnetization measurements. The samples were pre-annealed at 900°C for 10 min, which is in the ferrite/austenite two-phase region, and subsequently quenched to 400°C. Holding time at 400°C is 2 min for A11.8 grade steel or 1.5 min for Al1.0 grade steel, which was found to be close to the time leading to maximum volume fraction of retained austenite,[10,20] as also listed in Table 1.

Samples with a diameter of 5 mm and a thickness of about 1 mm were used for the thermo-magnetization measurements, which were performed on a Quantum Design SQUID magnetometer (MPMS-5S). During the measurements, the samples were thermally cycled from 300 to 5 K at a constant magnetic field of 5 T. Heating and cooling rates were very low (about 0.5 K/min) so that it can be assumed that the sample is in the equilibrium condition. The applied magnetic field is sufficiently large to approach the magnetic saturation according to previous investigations.[20] To analyze the chemical driving force for the martensitic transformation, the Gibbs free energy of austenite and martensite was calculated employing the computational thermodynamics program MTData® (version 4.71). The SGTE (Scientific Group Thermodata Europe) database was employed during the calculation.

In situ conventional X-ray diffraction (XRD) measurements under stress were performed on a Brucker D5005 X-ray diffractometer by means of a home-made tensile tester. After application of each stress step, a thin layer of standard silicon powder (NBS402) was pasted onto the sample surface to correct for the displacement of the surface during the tensile test by monitoring the shift of the {220} silicon peak. CoKα radiation was used at 45 kV and 35 mA and 2θ value is ranged from 45° to 95°. Three austenite (γ) peaks, $\{111\}_\gamma$, $\{200\}_\gamma$ and $\{220\}_\gamma$, and three ferrite (α) peaks, $\{110\}_\alpha$, $\{200\}_\alpha$, $\{211\}_\alpha$, were thus observed. From the net integral intensity and peak position, the volume fraction of retained austenite[21] and lattice parameters were thus calculated.

Table 1. Main chemical composition of the investigated steel (in wt%) and volume fraction of retained austenite, f_0^γ.

	C	Mn	Si	Al	f_0^γ
Al1.8	0.17	1.46	0.26	1.81	0.12
Al1.0	0.20	1.52	0.25	0.96	0.10

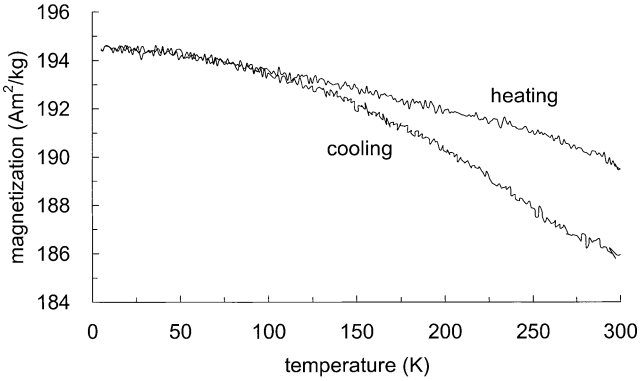

Fig. 1. Temperature dependence of mass magnetization in the Al1.0 grade steel during thermal cycle at a magnetic field of 5 T.

In situ synchrotron radiation measurements were performed at beamline ID-11 of European Synchrotron Radiation Facility (ESRF). A radiation beam with a size of $25\times25\ \mu m^2$ and a wavelength of 0.155 Å was applied. The diffraction patterns were detected by a charge-coupled device (CCD) with an exposure time of 30 s and an oscillation angle of 0.5°. The tensile samples have a thickness of 0.4 mm, a width of 10 mm and a gauge length of 50 mm, in which the length direction of the sample is parallel to the rolling direction. The tensile tests were performed on an Instron 25 kN stress-rig and the diffraction patterns were taken at strain levels ranged from 0 to 0.12.

3. Results and Discussion

3.1. Thermal Stability by Magnetization Measurements

Figure 1 depicts the mass magnetization as a function of temperature at a constant magnetic field of 5 T during the thermal cycle from 300 to 5 K and back in the Al1.0 grade steel. The magnetization increases significantly with decreasing temperature. This is due to, for the ferromagnetic phases, ferrite and martensite, the increase in the alignment of the atomic magnetic dipoles, and to the increase of martensite formed from retained austenite with decreasing temperature. From the results that the heating and cooling curves at low temperature level are coincident, one may see that nearly all retained austenite transforms to martensite after cooling, *i.e.* $f^\gamma \approx 0$. One can also understand that the volume fraction of ferrite remains unchanged during the thermal cycle, *i.e.* f^α=constant. The magnetization during cooling (M_c) and heating (M_h) is thus equal to M_c=

$f^{\alpha}\cdot M^{\alpha}+(1-f^{\alpha}-f^{\gamma})\cdot M^{\alpha'}$ and $M_h=f^{\alpha}\cdot M^{\alpha}+(1-f^{\alpha})\cdot M^{\alpha'}$. Denoting r as the ratio of the magnetization of martensite (α') and ferrite (α), $r=M^{\alpha'}/M^{\alpha}$, the temperature dependence of the austenite fraction during cooling can be determined by:

$$f^{\gamma}=\frac{M_h-M_c}{M^{\alpha'}}=\frac{M_h-M_c}{M_h}\cdot\frac{r+(1-r)f^{\alpha}}{r} \quad .....(2)$$

where the factor $(r+(1-r)f^{\alpha})/r$ arises from the difference of magnetization between the ferrite and martensite phase. The ratio r is here taken as 0.90, which is the literature data for an Fe–1.4C steel at room temperature.[22] f^{α} is estimated to be 0.85. Therefore, the austenite fraction as a function of temperature can be calculated, as shown by dots in **Fig. 2**. One can see that the austenite fraction decreases with decreasing the temperature as the transformation proceeds till the M_f temperature. However, the initial austenite volume fraction at 300 K is found to be only 0.023, which is much lower than expected.

To analyze the transformation behaviour in detail, the Gibbs free energy (G) of retained austenite and martensite was calculated. It is assumed that para-equilibrium is established during the heat treatment. Retained austenite has therefore an average composition of 1.40C–1.52Mn–0.25Si–0.96Al (in wt%), where the carbon concentration was determined from XRD.[23] From the Gibbs free energy, the chemical driving force for the martensitic transformation, $\Delta G=G^{\alpha'}-G^{\gamma}$, is obtained. Taking the critical driving force for the start of martensite transformation as 1 260 J/mol,[23] the M_S temperature is thus calculated to be 345 K. Furthermore, it is known that a magnetic field would assist martensitic transformation by giving an additional driving force of HM (H: applied magnetic field).[25] In a constant applied field of 5 T, this additional driving force is about 53 J/mol, which raises the M_S temperature by about 10 K. The M_S temperature is thus expected to be 355 K at a magnetic field of 5 T. Part of the retained austenite after the heat treatment therefore have transformed upon cooling to room temperature.

Another important information from the thermodynamic analysis is the calculation of the β values, the ratio of the slopes of the temperature dependence of the Gibbs free energy for martensite (α') and austenite (γ), which are around 0.8 and decrease slightly with decreasing temperature. The β values were used to predict the following fraction–temperature relation, which is slightly modified from a relation developed by H. Y. Yu[26]

$$f^{\gamma}=f_o^{\gamma}\left(1-\frac{M_S-T}{M_S-\beta M_f-(1-\beta)T}\right) \quad .....(3)$$

where f_o^{γ} is the austenite fraction at M_S, T the temperature. As shown in Fig. 2, the predicted results from this equation were found to be well consistent with the experimental results. If the f^{γ}–T curve is extrapolated to the M_S temperature, one can obtain that the austenite fraction at the end of bainitic holding is 0.035.

Assuming that the thermal stability of retained austenite is only microscopically related to the carbon concentration in austenite, the f^{γ}–T relation can be thus explained. The transition temperature of individual austenite grain with different carbon concentration (C%), M_S temperature, can be calculated using Andrews' empirical equation:[27]

$$M_S=766-425\times C\% \text{ (in K)} \quad .....(4)$$

where the constant 766 is calculated considering the alloying elements re-distribution during intercritical annealing.[23] The calculated C%–M_S relation is plotted in Fig. 2 and it can be understood from this relation that, for instance, at room temperature, the possible carbon contents in different austenite grains vary from 1.10 to 1.55 wt%. This is due to the fact that the austenite with lower carbon contents would have M_S temperature higher than room temperature and would transform to martensite and the austenite with higher carbon contents would start to transform at temperatures lower than 120 K. With decreasing temperature, the austenite grains with lowest carbon concentration transform first.

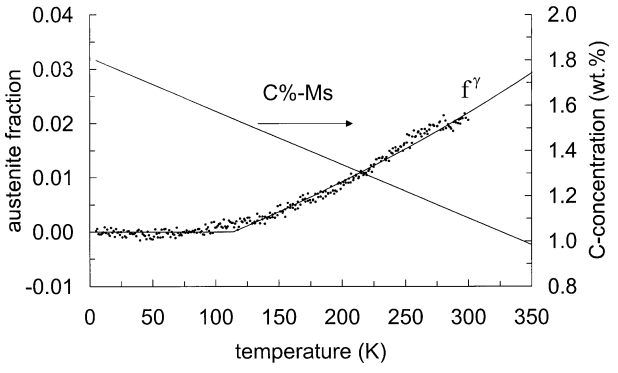

Fig. 2. Temperature dependence of austenite fraction during cooling. Dots represent the experimentally determined fraction using Eq. (2), and the solid line is the fitting of the dots using Eq. (3). Carbon concentration dependent M_S temperatures are calculated from Eq. (4).

3.2. Mechanical Stability Measured by Conventional XRD

From the *in situ* conventional XRD measurements at different strains, the volume fraction of retained austenite in the Al1.8 grade steel was determined, as shown in **Fig. 3**. The error bars indicated in the figure are those calculated from the counting statistics only.[20] Figure 3 confirms that Eq. (1) is also valid for the Al-containing TRIP steel investigated, that is, the auto-catalytic effect is suppressed due to the existence of ferrite and bainite surrounding the trans-

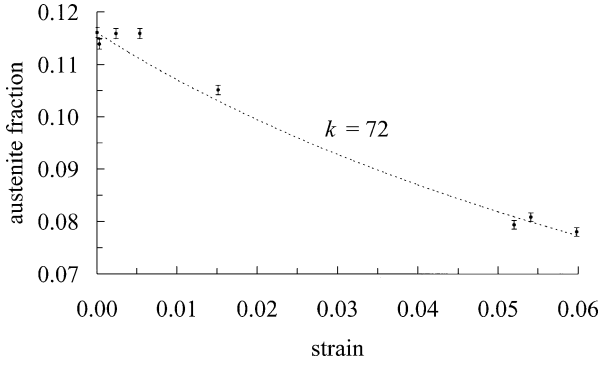

Fig. 3. Strain dependence of austenite fraction from *in situ* XRD measurements. The dotted lines are calculated from Eq. (1) with k=72.

forming austenite. Using Eq. (1), the k-value, regarded as a measure for the mechanical stability of retained austenite, is determined to be 72. In comparison with the k-values for the silicon containing TRIP steels[7,14,19] and dual phase steels,[14] the Al-grade steels are in general less stable than silicon-containing TRIP steels but much more stable than dual-phase steels.

The lattice parameter, a, of austenite was determined from the peak position of the $\{220\}_\gamma$ peak. The reason to choose this peak lies in the fact that the 2θ value of this peak is highest, which leads to highest accuracy. **Figure 4** shows the lattice parameter as a function of stress. One can see that the lattice parameter decreases with increasing stress. This is due to the fact that the diffraction plane is parallel to the sample surface, and tension along a direction parallel to the diffraction planes leads to a decrease of interplanar spacing of the diffraction planes. When the stress is less than 250 MPa, the lattice parameter decreases more or less linearly with increasing stress. However, when the stress is higher, the lattice parameter deviates from this linear relation. This is due to the fact that a significant fraction of austenite transforms to martensite as a result of stress- or strain-induced martensitic transformation. As analyzed below, the austenite with a lower carbon concentration is more likely to transform at lower stress values. As a consequence, the lattice parameter of remaining austenite shifts to values that are larger than given by the linear relation.

Assuming that there is no occurrence of the martensitic transformation at the stress below 250 MPa, the effect of stress on the parameter is thus extrapolated from the linear relation at the low stress levels to the maximum stress, as shown by a dotted line in Fig. 4. Subtracting this linear lattice parameter–stress relation from the measured values, the contribution of carbon to the austenitic lattice parameter is thus established using the following relation

$$a_C\,(\text{Å}) = 3.5980\,(\text{Å}) + 0.033\,C\,(\text{wt\%}) \quad \text{.....(5)}$$

where a_C is the austenitic lattice parameter only influenced by the carbon concentration (C) and the effect of other alloying elements (Al and Mn) is reflected in the constant of the relation above.[23] Carbon concentration as a function of stress is also plotted in Fig. 4, and one can see that the average carbon concentration increases from about 0.94 to 1.06% during the designed tensile test. From a thermodynamic point of view, this composition change means that there is only about 50 K decrease of the M_S temperature[27] or about 300 J/mol decrease of the chemical driving force.[4] Therefore, the XRD measurements show a small carbon concentration variation in the retained austenite.

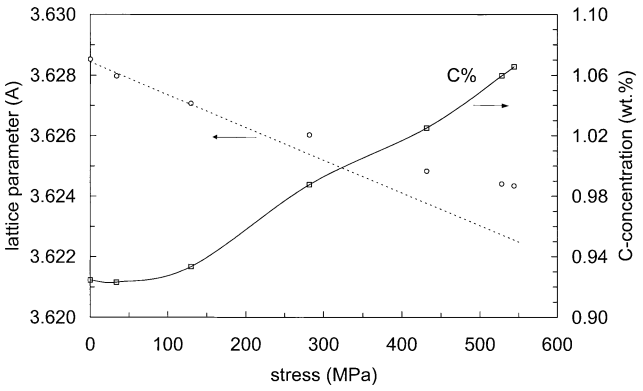

Fig. 4. Stress dependence of lattice parameter of austenite and carbon concentration in austenite.

3.3. Mechanical Stability Measured by Synchrotron Radiation

To understand the orientation effect on the mechanical stability of retained austenite, *in situ* synchrotron radiation measurements of the Al1.8 grade steel were performed in a stress rig. **Figure 5** shows an example of the measured diffraction pattern and the definition of the angle (η) between the normal of the diffracting plane and the direction of the applied stress. The first quarter of the austenite $\{200\}_\gamma$ diffraction ring, at which $2\theta \approx 4.9°$, was analyzed in this paper. The austenite fraction is determined from the relative inten-

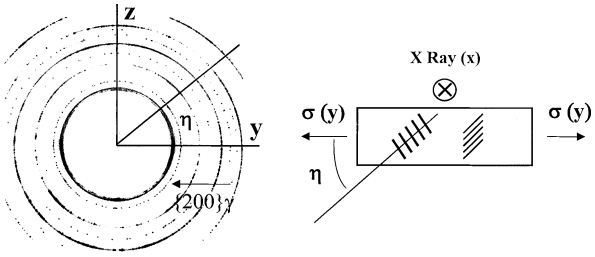

Fig. 5. An example of the diffraction pattern in the synchrotron measurements and schematic illustration of the definition of η-angle.

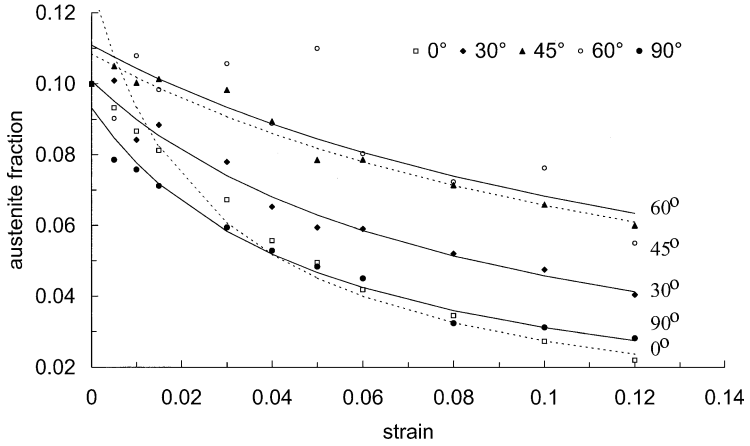

Fig. 6. Austenite fraction *versus* strain for different η-angles.

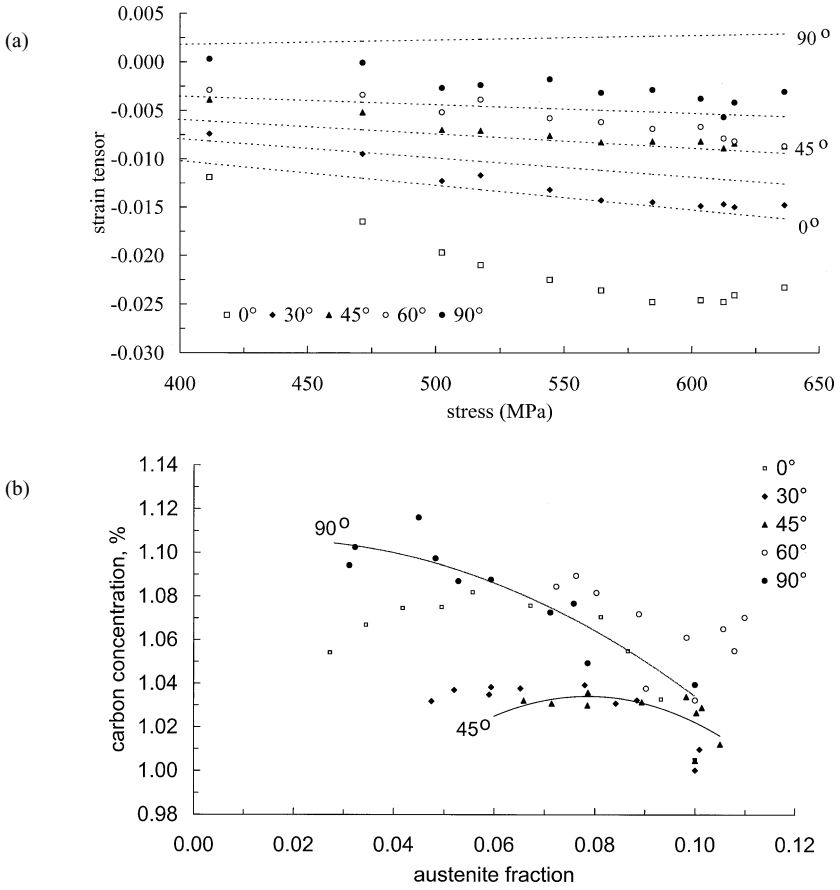

Fig. 7. (a) Stress-dependent strain tensor, predicated by Eq. (6) (dotted lines) and measured experimentally (symbols). (b) Carbon concentration *versus* the retained austenite fraction for different η-angles.

sity change and the fraction as a function of strain is shown in **Fig. 6**. The graph shows that the fraction of austenite decreases with increasing strain, except for a few points. Fitting the fraction *versus* strain relation in Fig. 6 by Eq. (1) with variable k and f_0^γ for different orientations, the k-values were obtained, as listed in **Table 2**. One can see that the retained austenite at η=0° or 90° is less stable and transforms preferentially while the austenite is most stable at η=45° or 60°. The mechanical stability at η=45° or 60° is close to the one by the conventional XRD measurements. The variation in f_0^γ indicates the presence of a texture for the retained austenite.

Similar to the analysis in the previous section, both stress and the carbon content in the retained austenite determine the interplanar spacing of the diffracting plane, which is proportional to the diameter of the diffraction ring. To calculate the stress (σ) effect, the following equation is derived[28)]

$$\varepsilon_2=\frac{(c_{11}+c_{12})\cos^2\eta-c_{12}\sin^2\eta}{(c_{11}+2c_{12})(c_{11}-c_{12})}\cdot\sigma \quad \text{.....(6)}$$

where c_{11} and c_{12} are the elastic constants. ε_2 is the strain tensor normal to the diffraction plane and is resulting from the change of interplanar spacing. Using c_{11}=217 GPa and c_{12}=145 GPa, the strain tensor is thus calculated and presented by the lines in **Fig. 7**(a), and one can see that the stress effect makes the diffraction ring have an oval shape, rather than an exact circle. From the relative values of the distance between the center and the edge of the diffraction ring, the strain tensor is also determined from the experimental data. After subtracting the stress effect on the strain tensor, the remaining strain is thought to be due to the change in the carbon content of the austenite. Therefore, the carbon concentration in remaining austenite is determined using Eq. (5) and the results are shown in Fig. 7(b). There is a significant trend that the carbon concentration increases for decreasing austenite fraction, in line with an expected increase in retained austenite stability with increasing carbon concentration. The variation in average carbon concentration is comparable to that obtained from the conventional XRD measurements.

Table 2. Orientation dependence of mechanical stability (k-values).

η	0°	30°	45°	60°	90°
k	364	120	65	62	199

4. Conclusions

In this work, both thermal and mechanical stability of retained austenite in TRIP steels are investigated by *in situ* X-ray measurements and thermo-magnetization measurements. Main conclusions can be drawn as follows.

(1) Both thermal and mechanical stabilities are mainly attributed to the fluctuations of carbon concentration among

different austenite grains. The austenite grains with a low carbon concentration transform more readily than grains with a higher carbon concentration.

(2) Thermo-magnetization measurements show that almost all austenite transforms to martensite upon cooling to 5 K and M_S and M_f temperatures are analyzed to be 355 and 115 K, respectively. Transformation kinetics on the fraction versus temperature relation were found to be well described by a model based on thermodynamics.

(3) From the *in situ* X-ray measurements, it is found that the volume fraction of retained austenite decreases as the strain increases according to Ludwigson and Berger relation, and the mechanical stability, characterized by the *k*-value, is strongly orientation-dependent.

Acknowledgements

The present authors thank Mr. O. Tegus and Dr. E. Brück for the thermo-magnetization measurements, Dr. L. Margulies and Dr. S. Grigull for the synchrotron radiation measurements and Ir. N. M. van der Pers for the conventional XRD measurements.

REFERENCES

1) O. Matsumura, Y. Sakuma and H. Takechi: *Trans. Iron Steel Inst. Jpn*., **27** (1987), 571.
2) K. Sugimoto, M. Kobayashi and S. Hashimoto: *Metall. Trans*., **23A** (1992), 3085.
3) F. D. Fischer, G. Reisner, E. Werner, K. Tanaka, G. Cailletaud and T. Antretter: *Int. J. Plast.*, **16** (2000), 723.
4) G. N. Haidemenopoulos and A. N. Vasilakos: *Steel Res*., **67** (1996), 513.
5) H. C. Chen, H. Era and M. Shimizu: *Metall. Trans*., **20A** (1989), 437.
6) O. Matsumura, Y. Sakuma, Y. Ishii and J. Zhao: *ISIJ Int*., **32** (1992), 1110.
7) A. Itami, M. Takahashi and K. Ushioda: *ISIJ Int*., **35** (1995), 1121.
8) P. Jacques, Q. Furnemont, A. Mertens and F. Delannay: *Philos. Mag*., **81A** (2001), 1789.
9) K. Sugimoto, M. Masahiro, M. Kobayashi and H. Shirasawa: *ISIJ Int*., **33** (1993), 775.
10) L. Zhao, J. Sietsma and S. van der Zwaag: Euromat 99, Vol. 7, ed. by P. Neumann, D. Allen and E. Teuckhoff, Wiley-Vch, Weinheim, (2000), 77.
11) M. de Meyer, D. Vanderschueren, K. de Blauwe and B. C. de Cooman: The 41st MWSP Conf. Proc., XXXVII, ISS/AIME, Warrendale, PA, (1999), 483.
12) O. Matsumura, Y. Sakuma and H. Takechi: *ISIJ Int*., **32** (1992), 1014.
13) L. Zhao, T. A. Kop, V. Rolin, J. Sietsma, A. Mertens, P. J. Jacques and S. van der Zwaag: *J. Mater. Sci*., **37** (2002), 1585.
14) O. Matsumura, Y. Sakuma and H. Takechi: *Scr. Metall*., **21** (1987), 1301.
15) J. B. Austin and R. L. Rickett: *Trans. Am. Inst. Min. Eng*., **135** (1939), 396.
16) T. Angel: *J. Iron Steel Inst*., (1954), 165.
17) D. C. Ludwigson and J. A. Berger: *J. Iron Steel Inst*., (1969), 63.
18) I. Tamura and C. M. Wayman: Martensite, ed. by G. B. Olsen and W. S. Owen, ASM International, Materials Park, OH, (1992), 231.
19) Y. Sakuma, O. Matsumura and O. Akisue: *ISIJ Int*., **31** (1991), 1348.
20) L. Zhao, N. H. van Dijk, E. Brück, J. Sietsma and S. van der Zwaag: *Mater. Sci. Eng*., **313A** (2001), 145.
21) C. F. Jatczak, J. A. Larson, S. W. Shin: Retained Austenite and Its Measurements by X-ray Diffraction, Society of Automotive Engineers, Inc., Warrendale, PA, (1980).
22) R. M. Bozorth: Ferromagnetism, D. van Nostrad Co. Inc, New York, (1951), 368.
23) L. Zhao, J. Moreno, S. O. Kruijver, J. Sietsma and S. van der Zwaag: Proc. Int. Conf. on TRIP-Aided High Strength Ferrous Alloys, ed. by D. C. de Cooman, Wissenschaftsverlag Mainz GmbH, Aachen, (2002), 141.
24) D. A. Porter and K. E. Easterling: Phase Transformations in Metals and Alloys, 2nd ed., Chapman & Hall, London, (1992), 387.
25) K. Shibata, T. Shimozono, Y. Kohno and H. Ohtsuka: *Mater. Trans. JIM*, **41** (2000), 893.
26) H. Y. Yu: *Metall. Mater. Trans*., **28A** (1997), 2499.
27) K. W. Andrews: *J. Iron Steel Inst*., (1965), 721.
28) L. Zhao and J. Sietsma: in preparation.